EUMETSAT

ROM SAF

RADIO OCCULTATION METEOROLOGY

Algorithm Theoretical Baseline Document: Level 2A refractivity profiles

Version 2.3

18 October 2021

ROM SAF Consortium
Danish Meteorological Institute (DMI)
European Centre for Medium-Range Weather Forecasts (ECMWF)
Institut d'Estudis Espacials de Catalunya (IEEC)
Met Office (METO)

Ref: SAF/ROM/DMI/ALG/REF/001

DOCUMENT AUTHOR TABLE

	Author(s)	*Function*	*Date*
Prepared by:	Stig Syndergaard	ROM SAF Design Coordinator	18/10 2021
Reviewed by (internal):	Johannes K. Nielsen	ROM SAF Scientist	21/02/2020
Approved by:	Kent B. Lauritsen	ROM SAF Project Manager	18/10 2021

DOCUMENT CHANGE RECORD

Version	*Date*	*By*	*Description*
1.0	28/02/2013	SSY	First version of ATBD for refractivity
1.1	16/03/2016	SSY	Version for PCR-RE1 review. New parts are Sections 2, 3.1, 3.3, 4, 5, 6, and 7.
1.2	12/08/2016	SSY	Updated version after PCR-RE1 review, taking into account RIDs #2, #7, #10, #11, #21, #22, #23, #26, #27, #28, #29.
1.3	23/02/2017	SSY	Internal version. Updated version reflecting changes in processing codes, configuration parameters, and QC as a result of tests before reprocessing RE1: - Section 3.2.2: Added sentences explaining the absence of further smoothing, which leads to consistency between raw and optimized bending; corrected sentence on assumed background error. - Removed previous section 3.2.3 regarding removal of L2 outliers in optimized bending angle. There is in practice no need for outlier detection at this point in the code, and no additional L2-extrapolation is needed. This part in the code is now avoided by setting a new configuration parameter opt_XL2 to false. The change is necessary to make raw and optimized bending angles consistent. - Section 3.3: Added line at end of section regarding assumed background error. - Section 4.2: Revised QC parameters and checks. - Section 6.1: Added explanation of difference to NRT as a consequence of the changes made to the reprocessing. - Section 7.2: Added opt_XL2 in section 5 of example configuration file.

1.4	11/06/2018	SSY	Version prepared for DRR-RE1 & ORR reviews. Updated version to be in line with the ATBD for bending angle after changes in pre-processing: - Section 4.2: Added sentence that refractivity is marked as non-nominal if bending angle or dry temperature is non-nominal. - Section 4.2: Added sentence about additional quality check at very high altitudes. - Section 7.2: Updated example configuration file. - Updated EUMETSAT logo.
1.5	31/08/2018	SSY	Updated version implementing the following RIDs from the DRR-RE1 & ORR review: - RIDs 047, 049, 052, 053, 057, 058, 059, 061, 062, 063, 070, 073, 074, 204, 205, 206, 207: Editorial/minor changes. In addition the following changes were made: - Included a few additional editorials provided by Barbara Scherllin-Pirscher.
1.6	20/12/2018	SSY	Updated version based on ICDR concept discussions at ROM SAF SG22: - Page 4: Update of the ROM SAF preface. - Table 1.1: Included ICDR products. - Section 1.4: New definitions of product types. - Section 6: Now referring to the new product types.
2.0	21/02/2020	SSY	Updated version for EPS-SG PDCR review: - Section 1.1: added Table 1.2 with EPG-SG products. - Section 1.1.1: New section on ROM SAF EPS-SG products. - Section 1.4: Modified NRT definitions for EPS-SG - Chapter 7: New chapter describing algorithm differences for EPS-SG products. Updated version for ORR12 review: - Table 1.1: Included GRM-60 and GRM 67 (Metop-C NRT and offline) - Section 3.1.1: Introduced f_1 and f_2 symbols for L1 and L2 frequencies - Section 3.2.2: New section on residual ionospheric correction. Subsequent section numbers increased by one. - Section 3.3: Modified to include residual ionospheric correction. - Section 6: Updated to reflect new difference between offline and CDR/ICDR processing.
2.1	15/05/2020	SSY	Updated version implementing the following RIDs from the ORR12 review: - RIDs 043, 098: Section 1.1: Removed text about future EPS-SG Day 1 products - RIDs 043, 098: Removed Section 1.1.1 and Chapter 7 about future EPS-SG Day 1 products - RID 042: Added Section 1.5 giving an overview of the remainder of the document

2.2	28/09/2021	SSY	Updated version submitted for the PCR review for Sentinel-6 NTC products implementing the following changes: - Section 1.1: Removed text to mention refractivity products in general and no specific version of PRD here; included GRM-117 in Table 1.1 - Section 1.3: Included NTC acronym - Section 1.4: Included NTC products - Section 1.5: Included NTC products - Section 3.1.1: Update to reflect that signal frequencies can vary depending on the GNSS constellation - Section 6: Included NTC products
2.3	18/10 2021	SSY	Updated version prepared during PCR review process implementing the following: - Sec. 1.4: Editorial corrections

ROM SAF

The Radio Occultation Meteorology Satellite Application Facility (ROM SAF) is a decentralised processing centre under EUMETSAT which is responsible for operational processing of radio occultation (RO) data from the Metop and Metop-SG satellites and radio occultation data from other missions. The ROM SAF delivers bending angle, refractivity, temperature, pressure, humidity, and other geophysical variables in near real-time for NWP users, as well as reprocessed Climate Data Records (CDRs) and Interim Climate Data Records (ICDRs) for users requiring a higher degree of homogeneity of the RO data sets. The CDRs and ICDRs are further processed into globally gridded monthly-mean data for use in climate monitoring and climate science applications.

The ROM SAF also maintains the Radio Occultation Processing Package (ROPP) which contains software modules that aid users wishing to process, quality-control and assimilate radio occultation data from any radio occultation mission into NWP and other models.

The ROM SAF Leading Entity is the Danish Meteorological Institute (DMI), with Cooperating Entities: i) European Centre for Medium-Range Weather Forecasts (ECMWF) in Reading, United Kingdom, ii) Institut D'Estudis Espacials de Catalunya (IEEC) in Barcelona, Spain, and iii) Met Office in Exeter, United Kingdom. To get access to our products or to read more about the ROM SAF please go to: http://www.romsaf.org

Intellectual Property Rights

List of Contents

1. Introduction

1.1 Purpose

This ATBD document describes the algorithms used to derive the refractivity products produced by the Radio Occultation Meteorology (ROM) Satellite Application Facility (SAF). The complete list of products covered by this ATBD is provided in Table 1.1[1]. Note that this table includes (or may include) both products in development and products with operational status. The status of all ROM SAF data products is available at the website: http://www.romsaf.org

The product requirements baseline is the PRD [AD.3]. The ATBD software package is based on the ROPP [RD.1].

Table 1.1 List of products covered by this ATBD

Product ID	Product name	Product acronym	Product type	Operational satellite input	Dissemination means	Dissemination format
GRM-01	NRT Refractivity Profile	NRPMEA	NRT Product	Metop-A Level 1B data from EUM Secretariat	GTS EUMETCast Web	BUFR BUFR BUFR/netCDF
GRM-09	Offline Refractivity Profile	ORPMEA	Offline Product	Metop-A Level 1A data from EUM Secretariat	Web	BUFR/netCDF
GRM-29-L2-R-R1	Reprocessed Refractivity Profile	RRPMET	Climate Data Record	Metop Level 1A data from EUM Secretariat	Web	BUFR/netCDF
GRM-29-L2-R-I1	ICDR Refractivity Profile	IRPMET	Interim Climate Data Record	Metop Level 1A data from EUM Secretariat	Web	BUFR/netCDF
GRM-30-L2-R-R1	Reprocessed Refractivity Profile	RRPCO1	Climate Data Record	COSMIC Level 1A data from CDAAC	Web	BUFR/netCDF
GRM-32-L2-R-R1	Reprocessed Refractivity Profile	RRPCHA	Climate Data Record	CHAMP Level 1A data from CDAAC	Web	BUFR/netCDF
GRM-33-L2-R-R1	Reprocessed Refractivity Profile	RRPGHA	Climate Data Record	GRACE Level 1A data from CDAAC	Web	BUFR/netCDF
GRM-40	NRT Refractivity Profile	NRPMEB	NRT Product	Metop-B Level 1B data from EUM Secretariat	GTS EUMETCast Web	BUFR BUFR/ BUFR/netCDF
GRM-47	Offline Refractivity Profile	ORPMEB	Offline Product	Metop-B Level 1A data from EUM Secretariat	Web	BUFR/netCDF
GRM-60	NRT Refractivity Profile	NRPMEC	NRT Product	Metop-C Level 1B data from EUM Secretariat	GTS EUMETCast Web	BUFR BUFR BUFR/netCDF

[1] Detailed information on the different input data types and their version numbers can be found in the validation reports at www.romsaf.org/product_documents.php.

Product ID	Product name	Product acronym	Product type	Operational satellite input	Dissemination means	Dissemination format
GRM-67	Offline Refractivity Profile	ORPMEC	Offline Product	Metop-C Level 1A data from EUM Secretariat	Web	BUFR/netCDF
GRM-117	NTC Refractivity Profile	ORPS6	NTC Product	Sentinel-6 Level 1B data from EUM Secretariat	Web	BUFR/netCDF

1.2 Applicable and reference documents

1.2.1 Applicable documents

The following list contains documents with a direct bearing on the contents of this document:

[AD.1] CDOP-3 Proposal: Proposal for the Third Continuous Development and Operations Phase (CDOP-3); Ref: SAF/ROM/DMI/MGT/CDOP3/001 Version 1.2 of 31 March 2016, Ref: EUM/C/85/16/DOC/15, approved by the EUMETSAT Council at its 85th meeting on 28-29 June 2016

[AD.2] CDOP-3 Cooperation Agreement: Agreement between EUMETSAT and DMI on the Third Continuous Development and Operations Phase (CDOP-3) of the Radio Occultation Meteorology Satellite Applications Facility (ROM SAF), Ref. EUM/C/85/16/DOC/19, approved by the EUMETSAT Council and signed at its 86th meeting on 7 December 2016

[AD.3] ROM SAF Product Requirements Document, Ref. SAF/ROM/DMI/MGT/PRD/001

1.2.2 Reference documents

The following documents provide supplementary or background information, and could be helpful in conjunction with this document:

[RD.1] The Radio Occultation Processing Package (ROPP) User Guide, Part III: Pre-processor module, Ref. SAF/ROM/METO/UG/ROPP/004

[RD.2] Gorbunov ME (2009) Upgrading of OCC code for operational processing of GRAS raw sampling data. ROM SAF CDOP Visiting Scientist Report 6, Ref: SAF/GRAS/DMI/MGT/CVS06/003

[RD.3] Gorbunov ME (2002) Canonical transform method for processing radio occultation data in the lower troposphere. Radio Sci. 37:1076, doi:10.1029/2000RS002592

[RD.4] Scherllin-Pirscher B, Syndergaard S, Foelsche U, and Lauritsen KB (2015) Generation of a bending angle radio occultation climatology (BAROCLIM) and its use in radio occultation retrievals. Atmos. Meas. Tech. 8:109-124, doi:10.5194/amt-8-109-2015.

[RD.5] Syndergaard S (2012) Deriving bending angle, refractivity, temperature, and

pressure using GRAS SAF software. Technical report (WP-2) of Assessment of the Structural Uncertainty of GRAS Products from Level 1B (bending angles) up to Level 2 (temperatures), Danish Meteorological Institute, EUMETSAT Contract No. EUM/CO/10/4600000745/AvE.

[RD.6] Gorbunov ME (2002) Ionospheric correction and statistical optimization of radio occultation data. Radio Sci. 37:1084, doi:10.1029/2000RS002370

[RD.7] Gorbunov ME, Shmakov AV, Leroy SS, Lauritsen KB (2011) COSMIC radio occultation processing: Cross-center comparison and validation. J Atmos Ocean Technol 28:737–751.

[RD.8] Hedin AE (1991) Extension of the MSIS thermosphere model into the middle and lower atmosphere. J. Geophys. Res. 96:1159-1172

[RD.9] Lauritsen KB, Syndergaard S, Gleisner H, Gorbunov ME, Rubek F, Sørensen MB, Wilhelmsen H (2011) Processing and validation of refractivity from GRAS radio occultation data. Atmos. Meas. Tech. 4:2065-2071, doi:10.5194/amt-4-2065-2011

[RD.10] Algorithm Theoretical Baseline Document: Level 1B bending angles, Ref. SAF/ROM/DMI/ALG/BA/001

[RD.11] Algorithm Theoretical Baseline Document: Level 2A dry temperature profiles, Ref. SAF/ROM/DMI/ALG/TDRY/001

[RD.12] The Radio Occultation Processing Package (ROPP) User Guide, part I: Input/Output module, Ref. SAF/ROM/METO/UG/ROPP/002

[RD.13] WMO FM94 (BUFR) Specification for Radio Occultation Data, Ref. SAF/ROM/METO/FMT/BUFR/001

[RD.14] Syndergaard S, Kursinski ER, Herman BM, Lane EM, Flittner DE (2005) A Refractive Index Mapping Operator for Assimilation of Occultation Data. Mon. Wea. Rev. 133:2650-2668. doi: http://dx.doi.org/10.1175/MWR3001.1

[RD.15] Syndergaard S (2012) Assessment of the Structural Uncertainty of GRAS Products from Level 1B (bending angles) up to Level 2 (temperatures), Final Report, Danish Meteorological Institute, EUMETSAT Contract No. EUM/CO/10/4600000745/AvE.

[RD.16] ROM SAF CDOP-2 Validation Report: Near Real-Time Level 2a Refractivity Profiles: Metop-A (GRM-01, NRPMEA) and Metop-B (GRM-40, NRPMEB), Ref: SAF/ROM/DMI/RQ/REP/001

[RD.17] Gorbunov ME, Lauritsen KB, Rhodin A, Tomassini M, Kornblueh L (2006) Radio holographic filtering, error estimation, and quality control of radio occultation data. J. Geophys. Res. 111:D10105, doi:10.1029/2005JD006427

[RD.18] Zeng Z, Sokolovskiy S (2010) Effect of sporadic E clouds on GPS radio occultation signals. Geophys Res Lett 37:L18817, doi:10.1029/2010GL044561

[RD.19] Sokolovskiy SV (2001) Tracking tropospheric radio occultation signals from low Earth orbit. Radio Sci 36:483-498

[RD.20] Sokolovskiy SV, Schreiner W, Rocken C, and Hunt D (2009) Optimal noise filtering for the ionospheric correction of GPS radio occultation signals. J. Atmos. & Oceanic Tech. 26:1398-1403, doi:10.1175/2009JTECHA1192.1

[RD.21] Ho SP, et al. (2012) Reproducibility of GPS radio occultation data for climate monitoring: Profile-to-profile inter-comparison of CHAMP climate records 2002 to 2008 from six data centers. J. Geophys. Res. 117:D18111, doi:10.1029/2012JD017665

[RD.22] Steiner AK, et al. (2013) Quantification of structural uncertainty on climate data

records from GPS radio occultation. Atmos. Chem. Phys. 13:1469-1484, doi:10.5194/acp-13-1469-2013

[RD.23] Culverwell I (2013) A review of the geodesy calculations in ROPP, Ref: SAF/ROM/METO/REP/RSR/014

[RD.24] Offiler D (2016) Simplifying EGM96 undulation calculation in ROPP, Ref: SAF/ROM/METO/REP/RSR/016

[RD.25] Healy SB, Culverwell, ID (2015) A modification to the standard ionospheric correction method used in GPS radio occultation. Atmos. Meas. Tech. 8:3385-3393, doi:10.5194/amt-8-3385-2015

1.3 Acronyms and abbreviations

ATBD	Algorithm Theoretical Baseline Document
BA	Bending Angle
BAROCLIM	Bending Angle Radio Occultation Climatology
BUFR	Binary Universal Format for data Representation
CDAAC	COSMIC Data Analysis and Archival Center
CDOP	Continuous Development and Operations Phase
CDR	Climate Data Record
CHAMP	Challenging Mini-satellite Payload
COSMIC	Constellation Observing System for Meteorology, Ionosphere, and Climate
DMI	Danish Meteorological Institute
ECMWF	European Centre for Medium-range Weather Forecasts
EGM96	Earth Gravitational Model
EPS	EUMETSAT Polar satellite System
EPS-SG	EPS Second Generation
EUMETSAT	EUropean organisation for the exploitation of METeorological SATellites
GNSS	Global Navigation Satellite System
GO	Geometric Optics
GPS	Global Positioning System (US)
GRACE	Gravity Recovery and Climate Experiment
GRAS	GNSS Receiver for Atmospheric Sounding (Metop instrument)
ICDR	Interim Climate Data Record
IEEC	Institut d'Estudis Espacials de Catalunya (Spain)
LEO	Low Earth Orbit
Metop	Meteorological Operational Polar satellite (EPS/EUMETSAT)
MSIS	Mass Spectrometer and Incoherent Scatter
MSL	Mean Sea Level
NCO	Numerically Controlled Oscillator
NetCDF	Network Common Data Form
NIMA	National Imagery and Mapping Agency
NRT	Near Real-Time

NTC	Non Time Critical
NWP	Numerical Weather Prediction
OLC	Optimal Linear Combination
PP	Pre-Processor
PRD	Product Requirements Document
QC	Quality Control
RMS	Root Mean Square
RO	Radio Occultation
ROM SAF	Radio Occultation Meteorology SAF (EUMETSAT), former GRAS SAF
ROPP	Radio Occultation Processing Package
SAF	Satellite Application Facility (EUMETSAT)
SNR	Signal-to-noise ratio
WGS84	World Geodetic System
WMO	World Meteorological Organisation
WO	Wave Optics

1.4 Definitions

RO data products from the Metop, Metop-SG and Sentinel-6 satellites and RO data from other missions are grouped in *data levels* (level 0, 1, 2, or 3) and *product types* (NRT, Offline, NTC, CDR, or ICDR). The data levels and product types are defined below[2]. The lists of variables should not be considered as the complete contents of a given data level, and not all data may be contained in a given data level.

Data levels:

Level 0: Raw sounding, tracking and ancillary data, and other GNSS data before clock correction and reconstruction;

Level 1A: Reconstructed full resolution excess phases, total phases, pseudo ranges, SNRs, orbit information, I, Q values, NCO (carrier) phases, navigation bits, and quality information;

Level 1B: Bending angles and impact parameters, tangent point location, and quality information;

Level 2: Refractivity, geopotential height, “dry” temperature profiles (Level 2A), pressure, temperature, specific humidity profiles (Level 2B), surface pressure, tropopause height, planetary boundary layer height (Level 2C), ECMWF model level coefficients (Level 2D), quality information;

Level 3: Gridded or resampled data, that are processed from Level 1 or 2 data, and that are provided as, e.g., daily, monthly, or seasonal means on a spatiotemporal grid, including metadata, uncertainties and quality information.

Product types:

[2]Note that the level definitions differ partly from the WMO definitions: http://www.wmo.int/pages/prog/sat/dataandproducts_en.php

NRT product: Data product delivered less than: (i) 3 hours after measurement (ROM SAF Level 2 for EPS); (ii) 150 min after measurement (ROM SAF Level 2 for EPS-SG Global Mission); (iii) 125 min after measurement (ROM SAF Level 2 for EPS-SG Regional Mission);

Offline and NTC products: Data product delivered from about 5 days to up to 6 months after measurement, depending on the applicable requirements. The evolution of this type of product is driven by new scientific developments and subsequent product upgrades;

CDR: Climate Data Record generated from a dedicated reprocessing activity using a fixed set of processing software[3]. The data record covers an extended time period of several years (with a fixed end point) and constitutes a homogeneous data record appropriate for climate usage;

ICDR: An Interim Climate Data Record (ICDR) regularly extends in time a (Fundamental or Thematic) CDR using a system having optimum consistency with and lower latency than the system used to generate the CDR[4].

1.5 Overview of this document

Chapter 2 gives a short algorithm overview, and Chapter 3 describes the technical details. Practical considerations such as validation method and quality control is given in Chapter 4, whereas assumptions and limitations are discussed in Chapter 5. Differences for NRT, Offline, NTC, CDR, and ICDR products are described in Chapter 6.

[3] (i) GCOS 2016 Implementation Plan; (ii) http://climatemonitoring.info/home/terminology/
[4] http://climatemonitoring.info/home/terminology/ (the ICDR definition was endorsed at the 9th session of the joint CEOS/CGMS Working Group Climate Meeting on 29 March 2018)

2. Algorithm overview

RO data may potentially have benchmarking quality for climate analyses because of the all-weather capability of the technique and because there is no need for calibration (as opposed to many other remote sensing instruments). However, RO processing is generally complex, not the least because different RO missions have different problems (such as low SNR, poor L2 tracking, data gaps, spikes, etc). Thus, besides the processing steps that can be easily described by equations, it is necessary to also have algorithms that can cope with a number of problematic issues. The algorithms in the Radio Occultation Processing Package (ROPP) have been developed over many years to do just that.

ROPP contains a module designed to compute ionospheric corrected bending angle, refractivity, and dry temperature profiles either from excess phase or L1 and L2 channel bending angle data derived from radio occultation measurements. A flow chart illustrating the ROPP pre-processor module is given in Figure 2.1. The main aspects of the algorithm for the Level 2A refractivity are described in the ROPP pre-processor user guide [RD.1].

The algorithm description in this ATBD complements the ROPP user guide by focusing on details not described in the user guide or elsewhere. References to equations and sections in the user guide are provided when appropriate. Many of the algorithms in the ROPP pre-processor module are also described in [RD.2]. References to original work on which algorithms are based are provided in the relevant sections.

In the descriptions in Section 3.2, the specific choices of parameters that affect the outcome of the processing are mentioned, such as filter widths, vertical grids, parameters determining specifics in the processing, interpolation methods, etc. The values mentioned are either hard-coded in the software or set in a configuration file in the ROM SAF processing. Although these choices have influence on the results, and contribute to the structural uncertainty of the products, they are not considered to have any negative impact on the products and they do not compromise the benchmarking quality of the data.

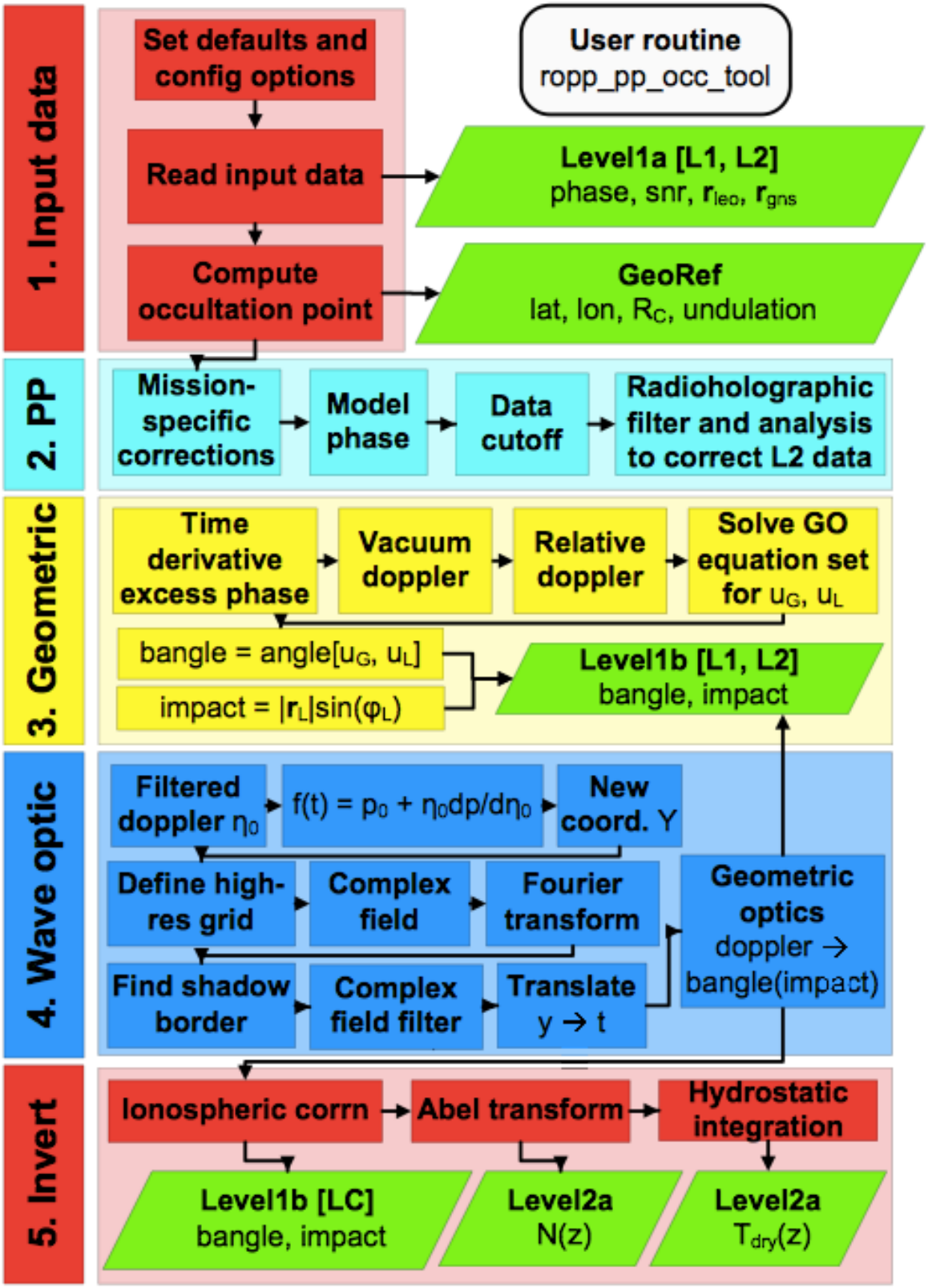

Figure 2.1 Flow chart illustrating calling tree of the ROPP pre-processor occ tool to compute ionospheric corrected bending angle, refractivity, and dry temperature profiles from input L1 and L2 channel amplitude and phase measurements [RD.1].

3. Algorithm description

3.1 Physics of the problem

3.1.1 Fundamental observables

The fundamental observables measured by an RO instrument are the phase, L_i, and amplitude, A_i, of the Doppler-shifted incoming signal. Index i denotes one of the two GNSS signals, L1 (at frequency f_1) and L2 (at frequency f_2). The signal frequencies can vary depending on the GNSS constellation. Each occultation measurement is a time-series of measured phases and amplitudes as well as precise position information for the transmitter (GNSS) satellite and the receiver (LEO) satellite.

3.1.2 Doppler-shift and derived quantities

The received signal is Doppler-shifted due to the motion of the transmitter and receiver satellites. With known satellite positions and velocities this Doppler-shift may be calculated to high precision for the vacuum case. When the ray bends in the atmosphere the angles between the ray path and the directions of motion are slightly different than in the vacuum case, both for the transmitting and the receiving satellite. This leads to a slightly different Doppler-shift. From observed signal phases, the observed Doppler-shift may be found and from this (with precise knowledge of the satellite positions and velocities) the bending of the ray path through the atmosphere may be derived. This leads to a profile of bending angles as a function of impact parameter. Via the Abel transform the profile of bending angles as a function of impact parameter is converted to a profile of atmospheric refractive index as a function of altitude. For convenience results are given in terms of the refractivity N instead of the refractive index n, with refractivity defined by $N = 10^6(n\text{-}1)$.

3.1.3 Ionospheric correction and statistical optimization

The bending of a ray passing through the atmosphere consists of a contribution from free electrons in the ionosphere, and a contribution from neutral species in the denser stratosphere and troposphere. The ionospheric contribution has a well-understood dependence on frequency whereas the neutral-atmospheric bending is approximately the same for the L1 and L2 frequencies. Therefore the presence of both the L1 and L2 signals allows one to disentangle the ionospheric contribution from the ionosphere-free or neutral-atmosphere contribution to the bending. The neutral-atmosphere contribution is the signal of interest in the present application, but in principle the algorithm also delivers the ionospheric signal as output. Because of measurement noise and residual ionospheric disturbances it is necessary to merge the measured bending angle with a very smooth background profile (usually from a climatology) at high altitudes (above some 40 km). This is referred to as statistical optimization.

3.2 Mathematical description of the algorithm

Given profiles of high-resolution L1, L2, and LC bending angles at equidistant impact parameter levels (cf. Section 3.2 in [RD.10]), the following subsections describe the steps taken to obtain the refractivity as a function of altitude above the geoid.

3.2.1 Background profile for statistical optimization

As a first step toward determining a background profile for the statistical optimization (cf. Section 3.1.3), a global search through a spectral representation of bending angles constructed from the BAROCLIM model [RD.4] is performed. The search goes through every month and every 10° latitude in the model (a total of 12x18=216 profiles). Each of these BAROCLIM bending angle profiles are compared with a smooth version (smoothed with a window corresponding to about 3 km; on a 100 m equidistant vertical grid) of the ionospheric corrected bending angle between 40 km and 60 km. The BAROCLIM bending angle profile with the best least squares fit (smallest RMS residual) is chosen to be modified to fit the ionospheric corrected bending angle even better (described in the next paragraph).

As a second step toward determining a background profile for the statistical optimization, the chosen BAROCLIM bending angle profile as a function of impact height is scaled by slightly different factors below 40 km and above 60 km, with a gradual transition in between. The mathematical details are described in [RD.5]. The resulting profile will in the following be referred to as the background profile. The scaling factors are found by linear regression as those which results in the closest fit between 40 km and 60 km. Usually the scaling factors are close to unity, but in cases of erroneous data, they can be off by large factors, and are therefore used as an additional quality check.

3.2.2 Residual ionospheric correction

The L1 and L2 bending angles, α_1 and α_2, as functions of impact parameter, a, are adjusted for residual ionospheric errors (cf. Section 3.2.20 in [RD.10]) such that they can be used in the following algorithms to obtain an ionospheric corrected and statistically optimized bending angle. The adjustments (denoted by an asterisk) can be written as

$$\alpha_1^*(a) = \alpha_1(a) - \frac{f_2^2}{f_1^2}\kappa(a)[\alpha_1(a) - \alpha_2(a)]^2$$

$$\alpha_2^*(a) = \alpha_2(a) - \frac{f_1^2}{f_2^2}\kappa(a)[\alpha_1(a) - \alpha_2(a)]^2$$

where $\kappa(a)$ is a slowly varying function of the impact parameter [RD.25], and based on a fixed Chapman profile for the ionospheric electron density. The Chapman profile has a scale height of 60 km and the electron density peak is fixed at a radius of 6670 km. For simplicity, the adjusted bending angles are referred to in the following as the L1 and L2 bending angles.

3.2.3 Dynamical error estimation

The principles of the dynamic error estimation for the statistical optimization are outlined in [RD.6] (cf. Section 4.5.2 in [RD.1]). The error estimation is based on certain vertical intervals. The upper limit that is used for the error estimation is determined as follows: First, the mean, μ, and standard deviation, σ, of the L1 and L2 bending angle difference between 12 km and 50 km is computed. The L1–L2 bending angle difference, ε, at any point above 50 km is considered too large if it is more than six standard deviations from the mean:

- if ε - μ > 6σ is found above 75 km, the upper limit is set to 70 km;
- if ε - μ > 6σ is found between 70 and 75 km, but not above, the upper limit is set to 65 km;
- if ε - μ > 6σ is found between 65 and 70 km, but not above, the upper limit is set to 60 km;
- if none of the above, the limit is set to 80 km;

The background profile is subtracted from the L1 and L2 bending angles, and the a priori ionospheric bending angle (in principle a smooth difference between L1 and L2 bending) is calculated using a sliding polynomial filter of degree three, and with a window width set to 50 m (Eq. 4.8 in [RD.1]). Since the bending angles are already smoothed to a much larger extent (about 3 km; see [RD.10]) and interpolated to a 100 m equidistant vertical grid, the setting of the window width to 50 m means in effect that the a priori ionospheric bending angle is not further smoothed.

The L1 and L2 bending angle noise (observation error) at high altitudes is estimated as the mean of the RMS of the standard ionosphere-free combination of the L1 and L2 bending angles (scaled by the frequencies squared) between 50 km and the upper limit, again using a sliding polynomial filter of degree three, and with a window width set to 50 m (Eq. 4.9 in [RD.1]). Again, this in effect means no further smoothing. The estimate of the error of the a priori ionospheric bending angle is also based on a mean between 50 km and the upper limit (Eq. 4.10 in [RD.1]). The assumed error of the background profile is fixed at 50%.

The absence of further smoothing as described above ensures that 'raw' and optimized bending angles will be consistent and only differ at high altitudes due to the influence of the background profile on the optimized bending angle.

3.2.4 Optimal Linear Combination (OLC)

The neutral atmospheric (statistically optimized) bending angle is given by optimal linear combination (OLC) [RD.6]. The OLC is solving a set of linear equations involving the L1 and L2 bending angles, the background profile, and the a priori ionospheric bending as determined above, as well as the estimated variances (Eqs. 2.40 and 2.41 in [RD.1]). The outcome is referred to as the OLC bending angle.

Above the top of the profile (uppermost data point), the OLC bending angle is augmented by the background profile up to 150 km. The combined profile is used later in the processing to refractivity, and will be referred to as the augmented OLC bending angle profile.

3.2.5 Abel transform

The augmented OLC bending angle profile is put through the Abel transform (Eq. 2.45 in [RD.1]) to obtain the refractive index and subsequently the refractivity as a function of impact parameter. With the Abel transform, the refractive index profile, $n(r)$, is given by

$$n(r) = \exp\left[\frac{1}{\pi}\int_x^\infty \frac{\alpha(a)}{\sqrt{a^2 - x^2}}\,da\right],$$

where α is the bending angle, a is the impact parameter, and $r = a/n(r)$. The Abel transform is implemented as a sum of contributions, assuming that bending angle varies linearly in between impact parameter levels (Eqs. 4.15 and 4.16 in [RD.1]). The level separation is equidistant and ~100 m.

3.2.6 Upper boundary condition

Above 150 km, the contribution to the Abel integral is determined by an expression assuming that the bending angle decreases exponentially with a constant scale height (Eq. 4.17 in [RD.1]). This is referred to as asymptotic correction. The scale height is determined from the uppermost 3/4 of the profile by a simple difference between the logarithm of the bending angle at 150 km and 115 km (equivalent to the mean slope of the logarithm of bending angle in this interval).

3.2.7 Conversion to Mean Sea Level (MSL) altitude

The altitude above the WGS84 ellipsoid is determined by the refractive index at a given impact parameter and the Earth's radius of curvature in the occultation plane (Eq. 2.3 in [RD.1]). The Mean Sea Level (MSL) altitude is calculated by subtracting the undulation. The undulation is based on the NIMA EGM96 geoid coefficients with respect to the WGS84 ellipsoid. These are in the form of geoid potential and correction coefficients to order and degree 360. The coefficients are expanded as Legendre polynomials and applied to the reference location of the occultation. The corresponding geopotential height is calculated using expressions derived from the Somigliana equation (see [RD.23] and [RD.24]).

3.3 Error sources

As a general consideration, the radio occultation signal consists of an excess phase and an amplitude. High-quality data is data with high SNR both in terms of amplitude and in terms of excess phase.

Amplitude noise is dominated by instrument noise under quiet ionospheric conditions. However, in the presence of ionospheric disturbances, or tilted sporadic E-layers, it can be severely affected by scintillations [RD.18]. Under quiet conditions the SNR is generally high except in the middle to lower troposphere, where the denser atmosphere leads to loss of signal intensity. This is particularly true when the humidity is high, which typically occurs in the tropics [RD.19]. This results in degraded bending angle data quality in the lower to middle troposphere, particularly in the tropics.

Besides instrument noise, the measured excess phase is affected by residual ionospheric noise [RD.20]. The ionospheric contribution to the signal is not fully removed by the ionospheric correction due to short timescale ionospheric variation and other higher order effects not accounted for in the residual correction. Since the measured excess phase signal is a function of atmospheric density it falls off approximately exponentially with impact height and so the noise comes to dominate the signal at high altitudes in the upper stratosphere and above. In the lower troposphere the tracking of the L2 signal becomes difficult and for that reason only the L1 signal is useful. This limits the accuracy of derived products.

The highest data quality is therefore found at intermediate altitudes of the higher troposphere to lower stratosphere, where the signal is strong both in terms of amplitude and in terms of excess phase.

Above a certain altitude in the upper stratosphere to lower mesosphere (depending on the noise level) the retrieved refractivity is based on a merge between observations and a climatology. The implementation of the global search and fitting procedure (Section 3.2.1), together with an assumed standard deviation of the background error of 50%, should ensure very little bias influence from the climatology.

4. Practical considerations

4.1 Validation method

As a whole, the algorithms are used to process a number of occultation observations, which are then compared to the corresponding profiles extracted from ECMWF analyses and forecasts (forward modelled to refractivity as a function of altitude above the geoid). The refractivity profiles based on input data from CDAAC are also compared to the corresponding refractivity profiles produced by CDAAC.

As the refractivity is derived from the bending angle, the validation of all parts of the processing chain from bending angle to refractivity is relevant to ensure the quality of the refractivity. Many parts of the algorithms described here together with those described in [RD.10] and [RD.11], have been validated over many years, as similar versions of the algorithms have been used to produce results for scientific publications and reports (see [RD.2], [RD.3], [RD.7], [RD.9], [RD.15], [RD.17], [RD.21], and [RD.22]).

Certain parts have been modified over the past few years in the version of ROPP at DMI. These parts include an improvement to the search and fitting strategy to find a suitable background for the statistical optimization and the development and inclusion of the BAROCLIM model (Section 3.2.1). These modifications were validated by comparisons to data produced by the unmodified code, comparisons against ECMWF analyses, and comparisons to corresponding profiles from CDAAC. The algorithms have also been validated by comparing 'raw' and optimized bending angles. The latter approach is an efficient way to evaluate to which extent a potential bias from the climatology affects the retrievals. The generation and the validation of BAROCLIM for its use in radio occultation retrievals (though with a different search and fitting strategy than the one used here) can be found in [RD.4].

4.2 Quality control and diagnostics

The following quality control parameters are used to ensure the quality of the refractivity products[5]:

L2 quality score:

Measures the quality of the L2 signal. This score is defined as the maximum of an L2 penalty function over the interval 25 km - 50 km (see [RD.10]). The L2 quality score is constructed such that a low value means high quality data.

Scaling factors:

The fitting of the background profile to the data at high altitudes results in two scaling factors. Usually the scaling factors are close to unity, but in cases of erroneous data, they can be off by large factors, and are therefore used as an additional quality check.

LC weighting function:

[5] Explicit numbers for the QC settings can be found in the validation reports at www.romsaf.org/product_documents.php

The LC weighting function determined individually for each profile in the statistical optimization is required to be sufficiently large below a given altitude (e.g., at least 0.9 at all altitudes below 40 km). The value indicates the fractional weight given to the data (as opposed to the background profile), and the weight increases rapidly downwards.

The L2 quality score, the scaling factors, and the LC weighting function are generated at different places in the code when the relevant parameters to generate them are readily available. They are output together with the data.

Besides checking the above quality control parameters, the following sanity checks are made to the data themselves:

- The independent variable (impact height for bending angle; altitude for refractivity and dry temperature) is required to vary monotonously.
- The bending angle and the refractivity are required to have valid values above and below certain impact heights/altitudes (e.g., above 60 km and below 20 km).
- At very high altitudes (e.g., above 60 km), the optimized bending angle is required to be within a certain threshold of the background profile used for statistical optimization.
- The refractivity is required to be positive at all altitudes (the generation of the dry temperature will fail if it is not).
- The bending angle and the refractivity are compared to the corresponding profiles extracted from an NWP model (forward modeled to refractivity and bending angle).

The refractivity is marked as non-nominal if any of the above checks results in parameters or data values outside defined thresholds. The refractivity is also marked as non-nominal if the incoming bending angle was marked as non-nominal, or if the processing to dry temperature results in non-nominal dry temperature [RD.11].

4.3 Outputs

The output of the processing to refractivity is a ROPP NetCDF file containing the following profile variables:

- Altitude above the geoid
- Geopotential height
- Refractivity

The same NetCDF file contains the output from the bending angle [RD.10] and dry temperature [RD.11] processing. A more complete and technical description of the output to the NetCDF file can be found in [RD.12].

The above-mentioned variables are also written to a BUFR file [RD.13].

5. Assumptions and limitations

5.1 Assumptions

5.1.1 Spherical symmetry

Radio occultation data are generally processed under the assumption of spherical symmetry. However, in principle this is only an apparent assumption because it depends on the interpretation of the retrieved profiles. If profiles are interpreted as representing the vertical structure in the atmosphere at a given fixed location, then the spherical symmetry assumption gives rise to a real error because the atmosphere is only approximately spherically symmetrical. If, on the other hand, retrieved profiles are interpreted as being weighted averages of the 3-dimensional (3D) atmosphere (primarily in the 2-dimensional (2D) occultation plane), the spherical symmetry assumption does not in principle give rise to any errors. This is why it could be an advantage to assimilate occultation data with 2D or 3D observation operators. A 3D observation operator for refractivity assimilation has been developed in [RD.14].

5.2 Algorithm limitations

The following subsections discuss limitations in the algorithms described in the corresponding subsections with the same titles in Section 3.2.

5.2.1 Dynamical error estimation

The dynamical error estimation results in a different weighting of the observations versus background in the statistical optimization for different occultations, which in turn gives differences in how far down into the stratosphere the background profile (climatology) is weighted significantly. An alternative approach (though not implemented in ROPP) would be to use a fixed (common for all observations) height interval for the transition between the observation and the background profile.

Retrieved refractivity profiles may occasionally (probably only a few times a month per satellite) be very bad with very large errors at high altitudes, with the error in some cases propagating all the way down to the surface. This is most likely related to the dynamical error estimation in combination with ionospheric scintillations at high altitudes (see RD.15]).

5.2.2 Optimal Linear Combination (OLC)

Vertical error correlations in observations and a priori are neglected in the statistical optimization.

6. Description of differences for NRT, Offline, NTC, CDR and ICDR products

This chapter describes the parts of the algorithm which are different for NRT, Offline, NTC, CDR and ICDR products[6].

6.1 NRT

The processing starts from Level 1B bending angles by transferring input files to a particular directory in the NRT operational system. The input bending angles are provided by EUMETSAT and are in the operational system pre-screened for cases with no or very few data points. Such input bending angles are then dismissed and not processed further.

Currently the statistical optimization is performed using MSIS [RD.8] instead of BAROCLIM, and the fitting and scaling approach follows that outlined in [RD.9] instead of that outlined in Section 3.2.1. A so-called MSIS bending angle profile is obtained for every month (one representative day), every 10° latitude, and every 20° longitude. A future upgrade of the NRT processing system will use BAROCLIM and the approach outlined in Section 3.2.1.

There is no residual ionospheric correction in the NRT processing.

The dynamical error estimation in the NRT processing is using other parameters than those described in Section 3.2.3, and there is an extra step correcting for outliers in the L2 bending angle below 12 km by additional L2-extrapolation. This makes the optimized bending angle different from the 'raw' bending angle provided by EUMETSAT, even at low altitudes.

Currently the code used in the NRT processing is not ROPP, but is a different set of Fortran libraries called OCC. However, the parts of ROPP used for processing radio occultation data was coded from OCC, and the two sets of algorithms and configuration parameters are mostly the same (except for the differences mentioned in this section). In a future upgrade the NRT processing will use the algorithms in ROPP as described in Section 3.

Since the NRT processing is based on input bending angles from EUMETSAT, the quality control (QC) in NRT is different from that described in Section 4.2 (see [RD.16] for a detailed account of the QC in NRT). In a future upgrade of the NRT processing system, the QC for NRT will become more in line with the QC described in Section 4.2.

6.2 Offline and NTC

The algorithms used for the Offline and NTC products are the ones described in Chapter 3.

[6] The impact of the different processings, as well as the impact of the different input data from providers, can be found in the validation reports at www.romsaf.org/product_documents.php.

6.3 CDR

The algorithms used for the CDR products are the same as the algorithms used in offline except for the residual ionospheric correction described in Section 3.2.2.

6.4 ICDR

The algorithms used for the ICDR products are the same as the algorithms used for the CDR products.

Appendices

A.1 Description of how to run the code

The code is run by the following command (for offline and reprocessing):

```
ropp_pp_occ_tool <input_file> --no-ranchk -o <output_file> -c
<config_file>
```

The input file is a ROPP NetCDF file containing high-resolution Level 1A data. The output file is a ROPP NetCDF file containing high-resolution Level 1B and 2A data.

The generation of a BUFR file is done by the following commands:

```
ropp2ropp <input_file> --no-ranchk -o <output_file> -p
<thin_file>
ropp2bufr <input_file> -o <output_file>
```

The input file to the `ropp2ropp` command is a ROPP NetCDF file containing Level 1B and 2A data (the high-resolution output of the retrieval). The output file of the `ropp2ropp` command is a ROPP NetCDF file containing thinned Level 1B and 2A data. The thinning file is the one provided by EUMETSAT (`ropp_thin_eum-247.dat`). The input file to the `ropp2bufr` command is the NetCDF file containing thinned Level 1B and 2A data and the output file is a BUFR file.

A.2 Configuration file

An example of a ROPP PP configuration file is given below. The values of parameters are not necessarily the final ones that will be set in the offline and reprocessing of refractivity.

```
# $Id: $

#****c* Configuration Files/metop_pp.cf *
#
# NAME
#    metop_pp.cf - METOP data configuration file for pre-processor
#    implementations in ROPP
#
# SYNOPSIS
#    <pp_program> ... -c metop_pp.cf ...
#
# DESCRIPTION
#    This file reflects the configuration for the PP
#    implementations within ROPP suitable for use with METOP data.
#
# NOTES
#
# AUTHOR
#   Met Office, Exeter, UK.
#   Any comments on this software should be given via the ROM SAF
#   Helpdesk at http://www.romsaf.org
#
# COPYRIGHT
#   (c) EUMETSAT. All rights reserved.
#   For further details please refer to the file COPYRIGHT
#   which you should have received as part of this distribution.
#
#****
```

```
#-------------------------------------------------------------------------------
# 0. Output options
#-------------------------------------------------------------------------------
output_lev1a = .false.      # Flag to output (modified) level 1a data

output_lev1b = .true.       # Flag to output level 1b data

output_lev2a = .true.       # Flag to output level 2a data

output_diag  = .true.       # Flag to output additional diagnostics

#-------------------------------------------------------------------------------
# 1. Excess phase to bending angle processing
#-------------------------------------------------------------------------------

# 1.1 Occultation processing method
# ---------------------------------

# GO - use GEOMETRIC OPTICS processing to derive bending angle as a function of
#      impact parameter from excess phase as a function of time.
# WO - use WAVE OPTICS (CT2 algorithm) processing to derive bending angle as a
#      function of impact parameter from excess phase as a function of time.

occ_method = WO

# 1.2 Filtering method
# --------------------

# optest - use OPTIMAL ESTIMATION: solution of integral equation
# slpoly - use SLIDING POLYNOMIAL

filter_method = slpoly

# 1.3 Smoothing bending angle profile
# -----------------------------------

fw_go_smooth = 3000.0  # Filter width for smoothed GO bending angles (m)

fw_go_full = 3000.0    # Filter width for full resolution GO bending angles (m)

fw_wo = 2000.0         # Filter width for wave optics bending angle above 7 km (m)

fw_low = -1000.0       # Filter width for wave optics bending angle below 7 km (m)

# 1.4 Maximum height for wave optics processing
# ---------------------------------------------

hmax_wo = 25000.0      # Maximum height for wave optics processing (m)

# 1.5 Data cut-off limits
# -----------------------

Acut     = 0.0         # Fractional cut-off limit for amplitude

Pcut     = -2000.0     # Cut-off limit for impact height

Bcut     = 0.1         # Cut-off limit for bending angle

Hcut     = -250000.0   # Cut-off limit for straight-line tangent altitude

# 1.6 CT2 options
# ---------------

CFF      = 3           # Complex field filter flag (CFF = 'Pa')

dsh      = 200.0       # Shadow border width (m)

# 1.7 Degraded L2 data flag
# -------------------------

opt_DL2  = .true.

# 1.8 Compute and output spectra flag
```

```
# ----------------------------------

opt_spectra = .false.

# 1.9 Paths to EGM96 geoid model coefficients and corrections file
# ----------------------------------------------------------------

egm96 = ../data/egm96.dat                 # EGM96 coefficients file

corr_egm96 = ../data/corrcoef.dat         # Correction coefficients file

#--------------------------------------------------------------------------------
# 1. Ionospheric correction processing
#--------------------------------------------------------------------------------

# 1.1 Ionospheric correction method
# ---------------------------------

# GMSIS - use MSIS climatology bending angle (searching global MSIS profiles
#         for best fit profile to obs) in ionospheric correction,
#         statistical optimization and bending angle to refractivity inversion.
#
# MSIS - use MSIS climatology bending angle in ionospheric correction,
#        statistical optimization and bending angle to refractivity inversion.
#
# GBARO - use BAROCLIM bending angle (searching global BAROCLIM profiles
#         for best fit profile to obs) in ionospheric correction,
#         statistical optimization and bending angle to refractivity inversion.
#
# BARO - use BAROCLIM bending angle in ionospheric correction,
#        statistical optimization and bending angle to refractivity inversion.
#
# BG   - use climatology from a specified input file containing
#        background temperature, pressure and humidity
#        (e.g. from an NWP analysis). The input filename can be specified
#        using the '-bfile' command line argument or setting 'bfile' (see 1.5).
#
# NONE - linear combination of L1 and L2 bending angles in ionospheric
#        correction, no additional information above observed profile top
#        in the inverse Abel to compute refractivity.

method  = GBARO               # Ionospheric correction method

# 1.2 Abel integral method
# ------------------------

# LIN  - assume linear variation of bending angle and ln(n) between
#        observation levels. This algorithm is used in ROM SAF NRT processing
#
# EXP  - assume exponential variation of bending angle and ln(n) between
#        observation levels. This algorithm is used in ropp_fm module.

abel = LIN

# 1.3 Statistical optimisation method
# -----------------------------------

# SO  - statistical optimisation.
# LCSO  - linear combination plus statistical optimisation.

so_method = so

# 1.4 Climatology model coefficients files
# --------------------------------

msisfile = ../data/MSIS_coeff.nc           # MSIS coefficients file for phase model
mfile    = ../data/BAROCLIM_coeff.nc       # Model coefficients file for stat. opt.

# 1.5 Background model temperature, humidity, pressure file
# ---------------------------------------------------------

bfile    = BG_file.nc       # Background meteorology profile file (method=BG)

#--------------------------------------------------------------------------------
```

```
# 2. Impact parameter grid
#------------------------------------------------------------------------------

# The ionospheric correction interpolates L1 and L2 bending angle profiles onto a
# standard grid.

dpi = 100.0            # Step of standard impact parameter grid (m)

#------------------------------------------------------------------------------
# 3. Smoothing bending angle profile
#------------------------------------------------------------------------------

# A smoothed bending angle profile is derived compute the fit of observed bending
# angles to the model bending angle profile.

np_smooth = 3          # Polynomial degree for smoothing regression

fw_smooth = 1000.0      # Filter width for smoothing profile

#------------------------------------------------------------------------------
# 4. Model bending angle profile fit to observations
#------------------------------------------------------------------------------

# To avoid systematic deviations from the observed profile with climatology,
# the model profile is scaled to the observed profile by a fitting method.

sf_method = regular     # Search and fit method (convoluted or regular)

nparm_fit = 2           # Number of parameters for model fit regression

hmin_fit  = 40000.0     # Lower limit for model fit regression

hmax_fit  = 60000.0     # Upper limit for model fit regression

omega_fit = 0.3         # A priori standard deviation of regression factor

#------------------------------------------------------------------------------
# 5. Ionospheric correction and statistical optimization
#------------------------------------------------------------------------------

# The method described by Gorbunov (2002) is implemented to perform ionospheric
# correction with statistical optimization.

f_width = 50.0         # Ionospheric correction filter width

delta_p = 100.0               # Step of homogeneous impact parameter grid

s_smooth = 50.0               # External ionospheric smoothing scale

z_ion = 50000.0               # Lower height limit of ionospheric signal

z_str = 35000.0               # Lower height limit of stratospheric signal

z_ltr = 12000.0               # Lower height limit of tropospheric signal

n_smooth = 11          # Number of points for smoothing (must be odd)

model_err = 0.5        # A priori model error std.dev. (dyn.est. if negative)

opt_XL2  = .false.      # L2 extrapolation on optimized bending angles

#------------------------------------------------------------------------------
# 6. Bending angle inversion to refractivity
#------------------------------------------------------------------------------

# The Abel inversion is computed to retrieve refractivity from corrected
# bending angles. The corrected bending angle profile is extended
# using MSIS or BAROCLIM data above the observed profile top.

ztop_invert = 150000.0 # Height of atmosphere top for inversion

dzh_invert = 50.0      # Step of inversion grid above observation top

dzr_invert = 20000.0   # Interval for regression in inversion
```

```
#------------------------------------------------------------------------------
# 7. Tangent point lat-lons
#------------------------------------------------------------------------------

# Set tp_bending=.true. to update lat-lons accounting for bending

tp_bending = .true.
```